Optics Letters

Designing high-performance nighttime thermoradiative systems for harvesting energy from outer space

Xin Zhang,[1] Jianying Du,[2] Jincan Chen,[2,4] Lay Kee Ang,[3] and Yee Sin Ang[3,5]

[1]School of Science, Jiangnan University, Wuxi 214122, China
[2]Department of Physics, Xiamen University, Xiamen 361005, China
[3]Science, Math and Technology, Singapore University of Technology and Design (SUTD), Singapore 487372, Singapore
[4]e-mail: jcchen@xmu.edu.cn
[5]e-mail:yeesin_ang@sutd.edu.sg

Received 16 June 2020; revised 9 September 2020; accepted 14 September 2020; posted 14 September 2020 (Doc. ID 400349); published 23 October 2020

Energy harvesting using thermoradiative systems has been extensively explored in recent years as a novel strategy for further reducing our energy footprint. However, the nighttime application, thermodynamic limit, and optimal design of such a system remain largely unaddressed so far. Here we propose an improved nighttime thermoradiative system (NTS) for electrical power generation by optically coupling Earth's surface with outer space. Our theoretical model predicts that the NTS operating with Earth (deep space) at 300 K (3 K) yields a maximum power density of 12.3 Wm^{-2} with an efficiency limit of 18.5%, which is potentially more advantageous than previous nighttime energy harvesting systems, such as a nighttime thermoelectric generator. We find that optimizing the thickness of the active layer, enhancing thermal infrared emission, and employing a silver backreflector for photon recycling are crucially important in improving system performance. This Letter provides new insights for the optimal designs of NTSs and paves the way toward practical nighttime power generation.

https://doi.org/10.1364/OL.400349

With the intensification of energy shortage and greenhouse effect, tremendous research attention has been paid to the development of practical renewable energy sources [1]. However, conventional photovoltaic cells (PVCs) can only generate electrical power during daytime [2]. The lack of nighttime performance undesirably necessitates the need for costly batteries and grid connection to other energy sources, such as fossil fuels. To continue the global push toward carbon neutrality, it is necessary to explore alternative sustainable energy technology that can efficiently generate electric power during nighttime.

The thermoradiative system (TS) represents an emerging technology for low-grade waste-heat recovery and radiative cooling [3,4]. Different from the operation of PVC under positive sunlight illumination, the TS operates at higher temperatures than the environment and radiates more photons than it absorbs to generate electric power under negative illumination [5]. Several pioneering works of the TS have been reported recently, mainly focusing on the theoretical efficiency limits [5–9], near-field radiative heat transfer [10–12], experimental demonstration [13–15], and renewable energy systems [16–18]. However, a thermoradiative (negative illumination) cell based on HgCdZnTe generates up to 1 pW of electrical power, which is insufficient for practical applications [14]. To improve the ability of power generation past the pW scale, radiative cooling utilizing the outer space as a cold reservoir could be a feasible approach to allow for a considerably larger temperature difference and power generation [19]. Despite being demonstrated as a promising way for nighttime energy harvesting, a rigorously theoretical model regarding the nighttime thermoradiative system (NTS) that includes the realistic optical and electric losses remains largely incomplete thus far. Quantifying the energy losses contributors, identifying the dominant loss mechanism that limits the power generation, and understanding the thermodynamic bounds and practical design strategies are some of the critical questions that urgently need to be addressed.

In this Letter, we propose a new design of the NTS that employs a mercury cadmium telluride ($Hg_{1-x}Cd_xTe$) p-n junction, and an Ag back surface reflector (BSR) under a parallel-plate geometry for efficient optical coupling between Earth and outer space to achieve nighttime energy harvesting. We construct a comprehensive model by considering two key irreversible processes of nonradiative and energy-dependent radiative loss. Moreover, the optical property, temperature dependence, and bandgap alignment of $Hg_{1-x}Cd_xTe$ are rigorously captured in our model, thus allowing a more realistic estimation of the theoretical power limit of our proposed NTS to be determined. We discuss the impact of these non-ideal mechanisms on system performance, and subsequently determine the optimal working conditions of the system. Our model shall form an important computational design basis for the technological implementation of practical NTSs, thus paving the way toward the efficient harvesting of renewable energy throughout the night.

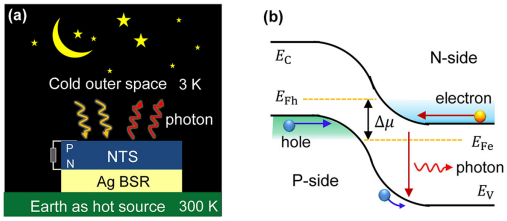

Fig. 1. (a) Schematic diagram of the nighttime thermoradiative system (NTS). (b) The band diagram of the transport route for carriers going through the NTS.

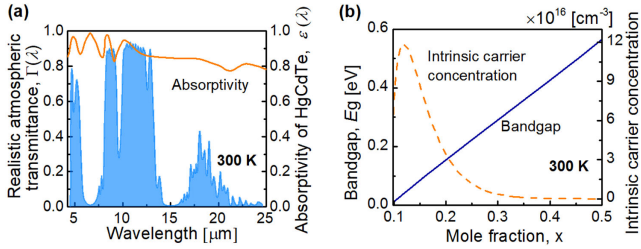

Fig. 2. Physical properties of $Hg_{1-x}Cd_xTe$. (a) The atmospheric transmittance and absorptivity varying with the wavelength; (b) bandgap and intrinsic carrier concentration varying with mole fraction.

As depicted in Fig. 1(a), a p-n-junction-based NTS relies on the thermoradiative effect and employs Earth as a heat source (300 K), and the darkness of space as a heat sink (3 K). Since the sky has an atmospheric transparency window ranging from 8 to 13 μm, the thermally emitted photons from the Earth's surface in this wavelength range can escape into outer space. Such a transparency window enables the NTS to access to the coldness of the outer space for electrical power generation via photon exchange, which forms the basis for all radiative cooling devices [20–22]. Figure 1(b) shows the transport routes of electrons and holes in the NTS. Thermally excited electrons in the n-side and holes in the p-side diffuse toward the space charge region and recombine radiatively over the bandgap, thus resulting in a negative open-circuit voltage. When a load is externally connected, the lack of electrons in the conduction band is replenished with equal holes current flow to the valence band, thus assuring a continuous charge flow through the NTS.

As an illustrative example, we consider the situation in which the temperatures of the Earth and deep space are maintained at 300 K and 3 K, respectively. Additionally, the effect of the realistic atmosphere condition is considered in our model. Since the high-melting materials with ultrahigh thermal conductivity are usually filled between them, we assume that the operating temperature of the NTS is the same as that of the Earth. Following the detailed balance formalism [23], the current density through such a device in terms of the difference between the emitted and absorbed photon fluxes, i.e.,

$$j_R = q[\Gamma(\lambda) N_{abs}(0,\ T_{Space}) - N_{em}(\Delta\mu,\ T_{Earth})], \quad (1)$$

where

$$N(\Delta\mu,\ T) = \frac{c}{4\pi}\int_{8\ \mu m}^{13\ \mu m} \varepsilon(\lambda) D(\lambda) \Theta(\Delta\mu,\ T) d\lambda. \quad (2)$$

Here q, λ, and c are the elementary charge, wavelength, and speed of light in vacuum, respectively. $\Gamma(\lambda)$ is the realistic atmospheric transmittance in the zenith direction [see Fig. 2(a)], which is obtained from MODTRAN5 [24]. $\varepsilon(\lambda)$ is the spectral absorption coefficient of the material surface. Here, $D(\lambda) = 1/(c\pi^2\lambda^2)$ is the photon density of states in a homogeneous bulk material. $\Theta(\Delta\mu,\ T) = [e^{(\hbar c/\lambda - \Delta\mu)/k_B T} - 1]^{-1}$ is the generalized Planck distribution, $\hbar$ is the reduced Planck constant, k_B is the Boltzmann constant, and $\Delta\mu = E_{Fe} - E_{Fh} = qV < 0$ is the chemical potential of photons. The current density given by Eq. (1) is related to the above bandgap photon flux, and its corresponding net radiative energy flux is given by

$$\dot{E}_{8\ \mu m<\lambda<13\ \mu m} = \dot{E}_{em}(\Delta\mu,\ T_{Earth}) - \dot{E}_{abs}(0,\ T_{Space}), \quad (3)$$

where

$$\dot{E}(\Delta\mu,\ T) = \frac{\hbar c^2}{4\pi}\int_{8\ \mu m}^{13\ \mu m} \frac{\varepsilon(\lambda) D(\lambda) f(\lambda,\ T,\ \Delta\mu) d\lambda}{\lambda}. \quad (4)$$

For endoreversible NTS under negative illumination, Buddhiraju *et al.* have reported the thermodynamic ultimate limit of power generation as follows [6]. The NTS has an outgoing heat flux equal to the net radiative flux between the ambient and the cold outer space; that is, $\dot{E}_{out} = \sigma(T_{Earth}^4 - T_{Space}^4)$, accompanied by the net entropy flux $S_{out} = (4/3)\sigma(T_{Earth}^3 - T_{Space}^3)$. Since the second law requires the input entropy flux S_{in} to be at most equal to S_{out}, the maximum heat flux that the NTS absorbed from the Earth is $\dot{E}_{in} = T_{Earth} S_{out} = T_{Earth} S_{in}$. Therefore, the maximum power density (MPD) that can be extracted is $P_{max} = \dot{E}_{in} - \dot{E}_{out} = T_{Earth} S_{out} - \dot{E}_{out} = T_{Earth}(4/3)\sigma(T_{Earth}^3 - T_{Space}^3) - \sigma(T_{Earth}^4 - T_{Space}^4)$, which is equal to 153.1 Wm^{-2} when the temperatures of the Earth and deep space are 300 K and 3 K [6]. This represents the ultimate limit for harvesting ongoing thermal radiation. Here, the volume and temperature of the NTS are assumed to be constant throughout the energy conversion process. The expression of $T_{Earth} S_{out} - \dot{E}_{out}$ is commonly referred to as the *exergy* of outgoing heat flow, that is, the maximum amount of work that can be extracted from an outgoing heat flow.

Here we choose $Hg_{1-x}Cd_xTe$ as the active p-n junction material in the NTS because of the following key characteristics: (i) the energy bandgap can be tailored made over the 1–30 μm range to be lower than thermal emission spectrum (8–13 μm), which contributes to more radiative photons and larger electrical currents [25]; (ii) $Hg_{1-x}Cd_xTe$ exhibits large optical coefficient and high electron mobility around 10^4 cm^2V^{-1} s^{-1} that enable high quantum efficiency [26]; and (iii) favorable inherent recombination mechanisms that allow high operating temperature. For a realistic NTS, the alignment of the material bandgap can appreciably affect the system performance. The bandgap $E_g(x,\ T)$ of $Hg_{1-x}Cd_xTe$ compounds at a given temperature T can be described as [27]

$$E_g(x,\ T) = E_{g0} + 1.93x - 0.81x^2 + 0.832x^3 + \alpha(1-2x)T, \quad (5)$$

where $E_{g0} = -0.302$ eV, and $\alpha = 5.35 \times 10^{-4}$. Furthermore, the nonradiative process, which serves as an additional loss

mechanism, shall affect the net free carrier generation in the NTS. To quantitatively describe the nonradiative loss, including the Auger and Shockley–Read–Hall (SRH) process, the net current losses generated in the NTS can be calculated as [25]

$$j_{\mathrm{NR}}(T) = qt\left[\frac{np-n_{\mathrm{i}}^2}{2n_{\mathrm{i}}^2}\frac{n}{(1+\beta n)\tau_{\mathrm{A}}}+\frac{1}{\tau_{\mathrm{SRH}}}\frac{np-n_{\mathrm{i}}^2}{n+p+2n_{\mathrm{i}}}\right], \tag{6}$$

where t denotes the thickness of the active region, n and p are the electron and hole concentrations, respectively. n_{i} is intrinsic carrier concentration. τ_{A} represents the intrinsic Auger recombination times, $\beta = 5.26\times10^{-18}\ \mathrm{cm}^3$, τ_{SRH} is the bulk Shockley–Read–Hall lifetime. The nonradiative recombination rate is a volumetric effect; thus, the number of nonradiative recombination events per unit area of the device is proportional to the thickness of the active layer, as shown in Eq. (6). Note that the thickness of $Hg_{1-x}Cd_xTe$ plays an important role in determining the performance of the NTS. On one hand, a large thickness enhances the wavelength-dependent absorption and emission from the $Hg_{1-x}Cd_xTe$ surface in accordance with the Kirchhoff law. As the number of emitted photons is much larger than those absorbed from the outer space, the power density increases. On the other hand, a small thickness strongly suppresses the nonradiative effect, which is strongly detrimental to the conversion efficiency [10]. Thus, an appropriate thickness is critically important for achieving good NTS performance. As a case study, we choose the inverse of the absorption coefficient ($10^5\ \mathrm{cm}^{-1}$) [25] as the $Hg_{1-x}Cd_xTe$ thickness, i.e., $t = 100$ nm, such that the $Hg_{1-x}Cd_xTe$ has sufficient thickness for photon absorption while remaining thin enough to mitigate the nonradiative effect. As demonstrated below, such a thickness leads to good conversion performance in the proposed NTS. We assume the NTSs are n-doped with a doping level of $1\times10^{15}\ \mathrm{cm}^{-3}$ and $\tau_{\mathrm{SRH}} = 1\ \mu\mathrm{s}$ based on the experimental measurements [25]. We also take into account the temperature dependence of n_{i} and τ_{A} [28],

$$n_{\mathrm{i}}(T) = (a - bx + lT - mxT)\times10^{14}E_{\mathrm{g}}{}^{3/4}T^{3/2}e^{-E_{\mathrm{g}}/2k_{\mathrm{B}}T}, \tag{7}$$

$$\tau_{\mathrm{A}}(T) = 8.3\times10^{-13}E_{\mathrm{g}}{}^{1/2}(q/k_{\mathrm{B}}T)^{3/2}e^{qE_{\mathrm{g}}/k_{\mathrm{B}}T}, \tag{8}$$

where $a = 5.585$, $b = 3.82$, $l = 0.001753$, $m = 0.001364$. In the following, we select an optimal mole fraction of 0.12 for $Hg_{1-x}Cd_xTe$. Such a value corresponds to a low bandgap of 0.05 eV that is below the atmospheric transparency window (i.e., 0.09 to 0.15 eV) and a maximum intrinsic carrier concentration of $1.8\times10^{17}\ \mathrm{cm}^3$, as shown in Fig. 2(b). Thus, thermally emitted photons from the Earth's surface with energies larger than the bandgap (0.05 eV) can escape into the outer space through the atmospheric transparency window, thus delivering larger electric currents and better system performances.

Considering the nonradiative process, in our proposed nighttime thermoradiative system, the total current density is given by

$$j = j_R - j_{NR}(T_{\mathrm{Earth}}), \tag{9}$$

and the output electrical power density and conversion efficiency of the NTS can be, respectively, expressed as

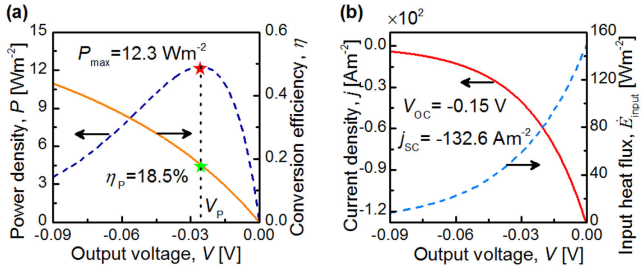

Fig. 3. Performance characteristics of the NTS operating between the Earth at 300 K and deep space at 3 K. (a) The P and η. (b) j and E_{Input} as functions of the negative output voltage V.

$$P = jV \tag{10}$$

and

$$\eta = \frac{P}{\dot{E}_{\mathrm{input}}} = \frac{jV}{P + \dot{E}_{8\ \mu\mathrm{m}<\lambda<13\ \mu\mathrm{m}}}. \tag{11}$$

As depicted in Fig. 1(a), the NTS emits the long-wave infrared spectrum into the outer space and simultaneously absorbs them from the outer space, thus producing the electrical power. Based on energy conservation, the absorbed heat $\dot{E}_{\mathrm{input}}$ from the heat reservoir (Earth) satisfies the relation in Eq. (11).

The performance characteristics of the system are sensitively dependent on the voltage output and chemical potential. Using Eqs. (1)–(11), we simulate realistically the performance characteristics of the system [Fig. 3]. The power density is a non-monotonous function of the output voltage [Fig. 3(a)], while the conversion efficiency decreases monotonously because the input heat flux increases with the output voltage [Fig. 3(b)]. The numerical results reveal that the system can generate a MPD of 12.3 Wm^{-2} for a voltage of −0.024 V, while yielding a corresponding efficiency of 18.5%. Although such an efficiency is far below the Carnot efficiency limit, the NTS still provides an equivalent figure of merit, $Z\bar{T}$, of 0.52, which is comparable to a high-performance thermoelectric generator (TEG). Here, the value of $Z\bar{T} = 0.52$ is calculated using Eq. (16) in Ref. [29] with $T_c = 3$ K, $T_h = 300$ K, and $\eta = 18.5\%$. Fig. 3(b) shows the volt-ampere characteristic curve of the NTS. The current density increases with the increment of the output voltage, and the system exhibits an open-circuit voltage of −0.15 V and a short-circuit current of $-132.6\ \mathrm{Am}^{-2}$.

We now identify the process that contributes to the major energy losses. The power generation and efficiency at different loss mechanisms are summarized in Table 1. The nonradiative and optical losses are two major loss mechanisms that significantly degrade system performance. Ongoing research efforts in suppressing the Auger effect via quantum wells, doping profile control, forming superlattices, and heterostructures, and mitigating the surface recombination by passivation will offer a pathway to quench the energy losses in the NTS. To reduce the optical loss, we propose that light-trapping surfaces with top dielectric grating and back metallic grating (Ag mirror) with high specular reflectivity can be integrated into the design of the NTS to promote light utilization.

It is important to note that the MPD and optimal values of the efficiency, current density, and output voltage closely depend on the heat source, i.e., the surface temperature of Earth. Adopting the MPD as the objective function, we find

Table 1. Quantification of Energy Loss Occurring in the NTS at 300 K

Parameter	Without Losses	With All Losses	Only Consider One Kind of Loss	
			Optical Loss	Nonradiative Recombination
P_{max} [Wm^{-2}]	18.6	12.3	17.2	13.7
η_P	23.8%	18.5%	21.8%	20.5%

Table 2. Comparison of Nighttime Energy Harvesting Systems Operating at 300 K

System	Photodiode under Negative Illumination[14]	TEG with Radiative Cooling[22]	NTS (Theoretical, This Work)
MPD	3 μW/m^2	0.025 − 0.5 W/m^2	12.3 W/m^2
Materials	HgCdZnTe	Semiconductor with $Z\bar{T} = 0.71$	HgCdTe

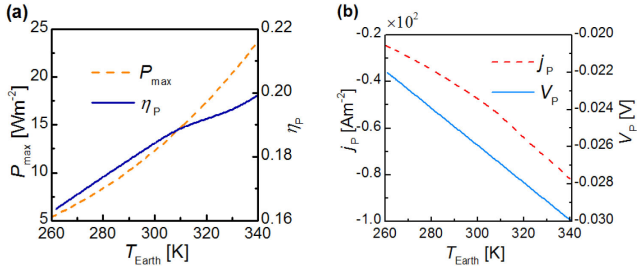

Fig. 4. Optimum values of (a) P_{max} and η_P; (b) j_P and V_P varying with the Earth's temperature.

that the MPD and the corresponding efficiency monotonically increase with the temperature in the range of 260 K to 340 K [see Fig. 4(a)]. However, the optimal values of the current density and output voltage decrease with the increase of the temperature, as shown in Fig. 4(b). This suggests that the trade-off among MPD, efficiency, current density, and output voltage must be carefully assessed when the NTS is operating at different ambient temperatures.

Finally, we briefly comment the potential advantages of the proposed system over other nighttime energy harvesting devices, as shown in Table 2, i.e.,the HgCdZnTe-based photodiode under negative illumination [14] and the TEG with radiative cooling [22], in which an MPD of 3 μW/m^2 and 0.025 − 0.5 W/m^2 has been experimental achieved, respectively. Here a commercial TEG (Marlow Industries TG 12-4) with $Z\bar{T} = 0.71$ is used, where the cold side is coupled to a simple black emitter facing the sky and the hot side is in direct contact with the environment [22]. The theoretically predicted MPD of the NTS, i.e., 12.3 W/m^2 when irreversible losses are included, is substantially higher than these systems, thus establishing the potential superior nighttime energy harvesting capability of our proposed system. The performance data of the NTS in Figs. 3 and 4 will offer an important design guideline for the implementations of high-performance NTSs to meet the varying demands of industrial and domestic energy conversions. Importantly, the predicted MPDs shall serve as a useful benchmark value for improving the experimental designs of NTSs in future experimental investigations.

In conclusion, we designed a high-performance $Hg_{1-x}Cd_xTe$-based nighttime thermoradiative system, which can directly harvest energy from the outer space via optical coupling with the Earth's surface. Based on our theoretical model, a 100 nm NTS yields a MPD of 12.3 Wm^{-2} when operating between the Earth at 300 K and the deep space at 3 K. Two major loss mechanisms are identified, namely the optical and nonradiative losses. Our results suggest that extensive design focus should be paid on enhancing the thermal infrared emission and integrating an Ag BSR. This Letter provides the realistic optimum design strategies for practical NTSs and will offer new insights in achieving efficient nighttime energy harvesting.

Funding. National Natural Science Foundation of China (11675132); Ministry of Education-Singapore (2018-T2-1-007).

Disclosures. The authors declare no conflicts of interest.

REFERENCES

1. S. Chu and A. Majumdar, Nature **488**, 294 (2012).
2. D. Li, J. Michel, J. Hu, and T. Gu, Opt. Lett. **44**, 3274 (2019).
3. J. Wang, C.-H. Chen, R. Bonner, and W. G. Anderson, in *AIAA Propulsion and Energy Forum* (2019).
4. X. Zhang, Y. S. Ang, J. Chen, and L. K. Ang, Opt. Lett. **44**, 3354 (2019).
5. R. Strandberg, J. Appl. Phys. **117**, 055105 (2015).
6. S. Buddhiraju, P. Santhanam, and S. Fan, Proc. Natl. Acad. Sci. USA **115**, E3609 (2018).
7. J. J. Fernández, J. Appl. Phys. **123**, 164501 (2018).
8. J. J. Fernández, J. Appl. Phys. **125**, 103101 (2019).
9. W. Li, S. Buddhiraju, and S. Fan, Light Sci. Appl. **9**, 1 (2020).
10. W.-C. Hsu, J. K. Tong, B. Liao, Y. Huang, S. V. Boriskina, and G. Chen, Sci. Rep. **6**, 34837 (2016).
11. S. V. Boriskina, J. K. Tong, W.-C. Hsu, B. Liao, Y. Huang, V. Chiloyan, and G. Chen, Nanophotonics **5**, 134 (2016).
12. J. J. Fernández, Eng. Res. Express **2**, 015040 (2020).
13. S. J. Byrnes, R. Blanchard, and F. Capasso, Proc. Natl. Acad. Sci. USA **111**, 3927 (2014).
14. P. Santhanam and S. Fan, Phys. Rev. B **93**, 161410 (2016).
15. M. Ono, P. Santhanam, W. Li, B. Zhao, and S. Fan, Appl. Phys. Lett. **114**, 161102 (2019).
16. T. Liao, X. Zhang, X. Chen, B. Lin, and J. Chen, Opt. Lett. **42**, 3236 (2017).
17. X. Zhang, Z. Ye, S. Su, and J. Chen, IEEE Electron Device Lett. **39**, 1429 (2018).
18. X. Zhang, Y. S. Ang, J. Y. Du, J. Chen, and L. K. Ang, J. Clean. Prod. **242**, 118444 (2020).
19. T. Deppe and J. N. Munday, ACS Photon. **7**, 1 (2019).
20. A. P. Raman, M. A. Anoma, L. Zhu, E. Rephaeli, and S. Fan, Nature **515**, 540 (2014).
21. E. Rephaeli, A. P. Raman, and S. Fan, Nano Lett. **13**, 1457 (2013).
22. A. P. Raman, W. Li, and S. Fan, Joule **3**, 2679 (2019).
23. W. Shockley and H. J. Queisser, J. Appl. Phys. **32**, 510 (1961).
24. A. Berk, G. P. Anderson, P. K. Acharya, L. S. Bernstein, L. Muratov, J. Lee, M. Fox, S. M. Adler-Golden, J. H. Chetwynd, Jr., M. L. Hoke, R. B. Lockwood, J. A. Gardner, T. W. Cooley, C. C. Borel, P. E. Lewis, and E. P. Shettle, Proc. SPIE **6233**, 508 (2006).
25. A. Rogalski, Rep. Prog. Phys. **68**, 2267 (2005).
26. M. P. Mikhailova, *Handbook Series on Semiconductor Parameters*, M. Levinshtein, S. Rumyantsev, and M. Shur, eds. (World Scientific, 1996), Vol. **1**.
27. G. L. Hansen, J. L. Schmit, and T. N. Casselman, J. Appl. Phys. **53**, 7099 (1982).
28. G. L. Hansen and J. L. Schmit, J. Appl. Phys. **54**, 1639 (1983).
29. G. J. Snyder and T. S. Ursell, Phys. Rev. Lett. **91**, 148301 (2003).